PHYSICAL REVIEW B **72**, 161303(R) (2005)

Spin dynamics in electrochemically charged CdSe quantum dots

N. P. Stern, M. Poggio, M. H. Bartl, E. L. Hu, G. D. Stucky, and D. D. Awschalom
Center for Spintronics and Quantum Computation, University of California, Santa Barbara, California 93106, USA
(Received 28 July 2005; published 6 October 2005)

We use time-resolved Faraday rotation to measure coherent spin dynamics in colloidal CdSe quantum dots charged in an electrochemical cell at room temperature. Filling of the $1S_e$ electron level is demonstrated by the bleaching of the $1S_e-1S_{3/2}$ absorption peak. One of the two Landé g factors observed in uncharged quantum dots disappears upon filling of the $1S_e$ electron state. The transverse spin-coherence time, which is over 1 ns and is limited by inhomogeneous dephasing, also appears to increase with charging voltage. The amplitude of the spin precession signal peaks near the half-filling potential. Its evolution at charging potentials without any observable bleaching of the $1S_e-1S_{3/2}$ transition suggests that the spin dynamics are influenced by low-energy surface states.

DOI: 10.1103/PhysRevB.72.161303 PACS number(s): 78.67.Hc, 78.47.+p, 71.35.Pq, 73.22.−f

In recent years, chemically synthesized semiconductor quantum dots (QDs) have been used in a wide variety of applications from QD lasers[1–4] and light-emitting devices,[5,6] to fluorescent labels.[7,8] The size-tunable spectrum of energy levels and the ease of colloidal nanocrystal synthesis make these nanocrystals versatile systems for the study of confined charges; the ability to optically excite carriers has spurred work on coherent spin dynamics in colloidal QDs revealing multiple Landé g factors and spin-coherence times reaching several nanoseconds at room temperature.[9,10] Advances in electrochemical charging of such nanocrystals have given researchers exquisite control over the electronic state of the QD and have opened new avenues in the study of state-filling effects in colloidal QDs (Refs. 11–13). In this paper we study the effects of electrochemical charging on the spin dynamics of optically excited carriers in an ensemble of CdSe QDs. The filling of QD energy levels affects properties such as the transverse spin lifetime and the Larmor precession frequencies, revealing the dependence of QD spin coherence on surface states and the externally controlled electron occupation.

Stearic acid capped 6-nm diameter CdSe nanocrystal QDs are synthesized and purified by standard colloidal chemistry methods[14] and are dissolved in a 9:1 (by volume) hexane: octane mixture. Following the methods of Guyot-Sionnest and co-workers,[12,13] close-packed CdSe nanocrystal films are formed by drop casting the QDs onto a quartz slide covered with a transparent indium-tin-oxide (ITO) electrode modified with 4-aminobutyl-dimethylmethoxysilane linker molecules. Dipping these films into a 5-mM solution of 1, 7-diaminoheptane in anhydrous methanol followed by a bake for 3 h at 70 °C cross-links the "loosely" packed QDs into tightly close-packed arrays. The nanocrystal-coated slide is then immersed in a 0.1-M electrolyte solution of tetrabutylammonium tetrafluoroborate dissolved in anhydrous N,N-dimethylformamide inside a fluorometer cell. A Pt counter-electrode and Ag pseudoreference electrode complete a three-terminal electrochemical cell with the ITO working electrode. The preparation of the QD film and assembly of the cell are conducted inside an argon atmosphere glove box. Before removal from the glove box, the cell is sealed with epoxy and enclosed within a vacuum-tight vessel to prevent oxidation; external feedthroughs connect the contacts within the vessel to a potentiostat which maintains a voltage V_{cell} between the reference and working electrodes. Negative V_{cell} injects electrons into the $1S_e$ state of the QDs, evidenced by bleaching of the $1S_e-1S_{3/2}$ interband absorbance peak measured using a white light source and a spectrometer.[13] After measurement at the desired V_{cell}, a positive bias of $V_{cell}=0.5$ V is applied in order to discharge the quantum-confined states and any long-lived localized trap states which may also have been filled. Repeated charging can cause the bleaching process to slow or eventually cease as oxygen or other impurities induce irreversible chemical reactions in the film and electrolyte. Careful fabrication of the cross-linked QD film and assembly of the air-tight electrochemical cell are critical for a sample with long-lived reproducible charging behavior.

Typical optical absorbance spectra $\alpha(E)$ are shown in Fig. 1(b), showing the $1S_e-1S_{3/2}$ absorption peak bleaching with negative V_{cell}. The bleaching spectrum is calculated as $(\alpha-\alpha_0)/\alpha_0$, where α is the film's absorption at a given V_{cell} and α_0 is the absorption for $V_{cell}=0$ V, and is shown in Fig. 1(c) for representative values of V_{cell}. The average number of electrons occupying the $1S_e$ state in the QD ensemble can be

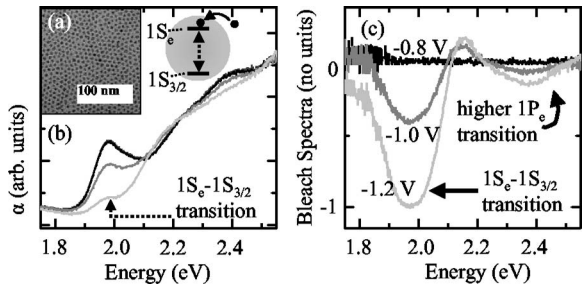

FIG. 1. (a) TEM image of a close-packed CdSe nanocrystal film. (b) Absorbance spectra $\alpha(E)$ at $V_{cell}=-0.8$ V (black), −1.0 V (gray), and −1.2 V (light gray) along with a schematic of relevant energy levels in charging experiments. $V_{cell}=0.0$ V is identical to $V_{cell}=-0.8$ V. (c) Bleaching spectra relative to $V_{cell}=0.0$ V as described in the text. Bleaching of the $1P_e$ electron level can be seen at 2.35 eV.

controlled between 0 and 2 with the appropriate V_{cell} so that the degree of bleaching has a direct relation to the occupation of the $1S_e$ state.[13] V_{half} corresponds to an average electron occupation of 1 in the $1S_e$ state of each quantum dot and $(\alpha-\alpha_0)/\alpha_0=0.5$. V_{half} varies from -0.85 to -1.0 V between QDs with nominally similar sizes due to variations in cell assembly and film quality. Bleaching of the $1S_e-1S_{3/2}$ transition occurs over a range of ± 0.1 V around V_{half}.

Coherent spin dynamics are measured by time-resolved Faraday rotation (FR) in the Voigt geometry.[15] A mode-locked 76-MHz Ti:sapphire laser pumps an optical parametric oscillator, producing 200-fs pulses tunable between energies of 1.97 and 2.21 eV which are split into a circularly polarized 1-mW pump and linearly polarized 30-μW probe beam. We also use a regeneratively amplified Ti:sapphire laser to pump two optical parametric amplifiers (OPA) allowing independent tuning of pump and probe energies. The dual OPA system improves signal to noise, but the qualitative features of the FR were unchanged between laser systems. The pump helicity is varied at 40 kHz by a photoelastic modulator, while the probe beam is chopped at 1 kHz for lock-in detection. Both beams are focused to an overlapping 100-μm diameter spot on the QD film which is positioned between the poles of two permanent magnets. The pump pulse excites spin-polarized electron-hole pairs at time $t=0$, which we assume relax to the lowest-energy exciton state within a picosecond.[1,16,17] The pump-excited spins precess about the applied magnetic field B at the Larmor frequency $\nu_L=g\mu_B B/h$, where g is the Landé g factor, μ_B is the Bohr magneton, and h is Planck's constant. By the Faraday effect, the probe beam polarization axis rotates by an angle θ_F proportional to the spin polarization along the beam path; this angle is measured as a function of the time delay t between pump and probe pulses. For consistency, all reported FR measurements are at room temperature with $B=0.28$ T from a single film with $V_{\text{half}}=-0.95$ V. Variations in charging behavior between different samples due to nanocrystal size variation and sample quality make direct quantitative comparison between any two samples difficult, although the qualitative results from all samples measured agree with those reported here.

Figure 2 shows typical time-resolved FR time scans [Figs. 2(a)–2(d)] and the corresponding Fourier transforms [Figs. 2(e)–2(h)] for representative charging voltages with the pump and probe energies tuned to the $1S_e-1S_{3/2}$ exciton resonance in this sample at 2.03 eV. The data for $V_{\text{cell}}=0.0$ V are characterized by an oscillating component superimposed on a decaying background. The Fourier transform for this voltage [Fig. 2(e)], reveals two distinct frequencies (ν_1,ν_2) contributing to the oscillation, consistent with previous FR studies of CdSe QDs (Refs. 10 and 17). On charging, the FR amplitude increases while the relative weight of the higher-frequency component (ν_2) decreases until disappearing completely around V_{half} [Figs. 2(f)–2(h)]. The amplitude of the lower-frequency component (ν_1) decreases beyond V_{half}. Monitoring the absorbance of the probe beam, α_{probe}, ensures that the QDs within the laser focus spot are charging with the application of V_{cell} as the absorbance peak bleaches [Fig. 3(a)].

In order to more carefully examine these parameters, the

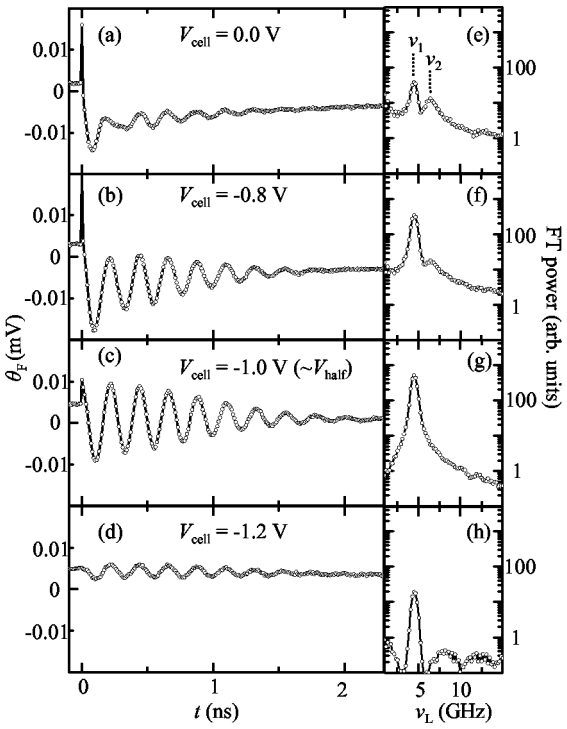

FIG. 2. (a)–(d) FR time-domain scans for representative voltages. Voltages not plotted represent a smooth evolution between the displayed results. The fast Fourier transforms in (e)–(h), which have been smoothed for clarity, show two frequencies in uncharged nanocrystals evolving to a single precession frequency in the charged ensemble.

FR time-domain data are fit to two decaying cosinusoidal components, given by Eq. (1),

$$\theta_F = \theta_0 + \theta_1 \exp(-t/T_{2,1}^*)\cos(2\pi\nu_1 t + \phi_1) + \theta_2 \exp(-t/T_{2,2}^*)\cos(2\pi\nu_2 t + \phi_2) + \theta_{\text{exp}} \exp(-t/\tau), \quad (1)$$

where θ_0 is an offset, $\theta_1(\theta_2)$ the amplitude of the first (second) frequency component, $T_{2,1}^*(T_{2,2}^*)$ the transverse spin-

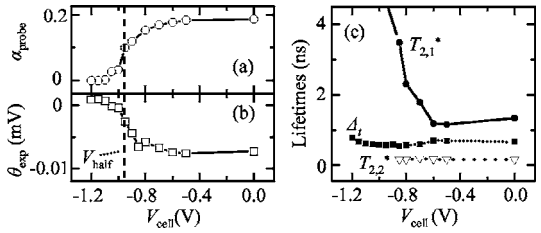

FIG. 3. (a) Absorbance of the probe beam, measuring the local bleaching at the laser focus spot. (b) Amplitude of the nonoscillating component θ_{exp}, which vanishes on charging. (c) Fit results for the spin-coherence times $T_{2,1}^*$ (circles), $T_{2,2}^*$ (triangles), and the Gaussian dephasing time Δ_t (squares). For $T_{2,1}^* \gg \Delta_t$, the fitting algorithm cannot quantitatively distinguish between a purely Gaussian lifetime and the exponential lifetime $T_{2,1}^*$, suggesting that the spin relaxation is completely dominated by inhomogeneous dephasing for $|V_{\text{cell}}|>1.0$ V.

coherence time, $\nu_1(\nu_2)$ the Larmor frequency, $\phi_1(\phi_2)$ the phase, θ_{exp} and τ the amplitude and decay time, respectively, of the nonoscillating exponential background. At voltages $V_{\text{cell}}<-0.9$ V, the second frequency component (ν_2) is not present and only one of the cosinusoidal terms is kept in the fit function.

The nonoscillating component with a decay time of $\tau=0.9\pm0.1$ ns disappears when the film is charged beyond V_{half} [Fig. 3(b)]. The origin of this component is unclear, as earlier studies of confined nanostructures have attributed similar nonoscillating signals to the decay of hole spins pinned along the growth axis,[15] the leakage of the longitudinal spin-relaxation signal,[10] surface carrier trapping,[9] or the decay of nonoscillating exciton populations.[18] The quenching of θ_{exp} with charging is consistent with the latter two explanations.

The lower-frequency FR amplitude θ_1 decays with a Gaussian envelope, indicating that the relaxation of coherent spins in the QD ensemble is dominated by inhomogeneous dephasing. The effect of the inhomogeneous QD size can be modeled as a Gaussian distribution of g factors with width Δ_g. Averaging the FR contributions over the ensemble introduces an additional Gaussian envelope to the oscillatory terms of Eq. (1) with a width $\Delta_t=\hbar/\mu_B B\Delta_g$ (Ref. 10). Fits to the FR yield both the Gaussian decay width and the transverse spin lifetimes [Fig. 3(c)]. Since Δ_t is about 0.7 ns for all V_{cell}, the dephasing is due to structural properties such as orientation and size variation that are not affected by changes in electronic occupation. Assuming all inhomogeneities are size related, this dephasing rate corresponds to a g-factor width $\Delta_g=0.06$ and a size distribution of about 15%. The size distribution of the synthesized QDs is estimated to be closer to 5%, suggesting contributions to the inhomogeneous broadening by shape anisotropy and random nanocrystal orientation for which this simple size-averaging procedure does not account. The spin-coherence time of the ν_1 component, $T_{2,1}^*$, increases dramatically with charging, though quantitative fit results for coherence times above 2 ns are not reliable because of the vanishing of the FR signal due to dephasing. This result is consistent with the large increase in spin lifetimes reported in n-doped self-assembled InAs-GaAs QDs compared to undoped QDs (Ref. 19). Further experiments in systems with less inhomogeneity or on single quantum dots will help avoid the limitations of inhomogeneous broadening and isolate the effects of charging upon the spin lifetime.

The amplitudes of the two FR components behave quite differently from each other [Fig. 4(a)]. The lower-frequency amplitude θ_1 increases significantly, reaching a maximum near V_{half} before decreasing toward zero in doubly charged QDs. θ_2 vanishes sharply at V_{half} due to the presence of charges in the $1S_e$ state.

Comparison between Figs. 3(a) and 4(a) show that θ_1 increases at V_{cell} well below the $1S_e$ charging near V_{half}. The amplitude increase between 0 V and V_{half} may be due to the filling of low-energy surface states on the nanocrystals which have been shown to provide fast nonradiative pathways for carrier relaxation. Surface defect states in uncharged QDs, in addition to influencing energy levels[20] and photoluminescence dynamics,[13] account for the relaxation of up to half of optically injected carriers within a few ps [Fig. 4(c)].[1,21] For

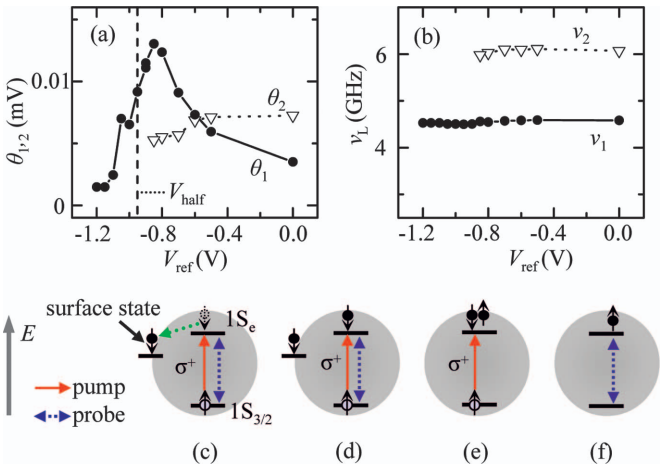

FIG. 4. (Color) (a) FR amplitudes θ_1 and θ_2 as functions of V_{cell}. (b) Larmor precession frequencies ν_1 and ν_2 corresponding to g factors of $g_1=1.15$ and $g_2=1.63$. (c)–(f) Schematic diagrams of charged QD spin dynamics under σ^+ pump excitation. For σ^- pump pulses, all spin directions should be reversed. (c) In a fraction of CdSe QDs, optically injected electrons relax nonradiatively (green arrow) into surface defect states within a few ps, leaving no $1S_e$ electron to probe. (d) For a V_{cell} that fills the surface states, optically injected electrons remain in the $1S_e$ level and FR can be measured in all QDs. (e) A circularly polarized pump pulse can only create an exciton in a charged QD with one spin orientation of the electrically injected charge. The singlet in the $1S_e$ state prevents probe pulses from interacting with this QD. (f) Probe pulses can measure a singly charged QD which has not absorbed a pump pulse; there is no exciton precession, however.

V_{cell} between 0 V and V_{half}, these empty surface states in the QD band gap can be filled by electrochemically injected charges, blocking the relaxation pathway and increasing the number of QDs in the ensemble with long-lived coherent electron populations [Fig. 4(d)]. This interpretation is supported by the disappearance in charged QDs of the spikes in the FR near $t=0$ which may denote decay processes on the order of a few ps [Figs. 2(a)–2(d)]. The FR amplitude reduction for charging beyond V_{half} is due to Pauli blocking of absorptive $1S_e-1S_{3/2}$ transitions, as evidenced by the commensurate bleaching [Fig. 1(c)] and reduction in probe beam absorption [Fig. 3(a)] in this regime.

The two constant precession frequencies [Fig. 4(b)] correspond to Landé g factors of $g_1=1.15$ and $g_2=1.63$, in agreement with what would be expected for a 6-nm diameter QD (Ref. 9). The origin of the two g factors in CdSe QDs has been attributed to multiple sources in the literature.[22] Theoretical calculations from effective mass models suggest that the lower-frequency g_1 is electron-spin precession.[10,23] Reference 10 follows this assignment and subsequently attributes g_2 to exciton precession in a subset of quasispherical QDs where the spin splitting due to shape and wurtzite crystal anisotropies cancel. Another interpretation of the time-resolved FR data in Ref. 10 proposed by Chen and Whaley[24] attributes the two observed g factors to the two anisotropic components of the g tensor $g_\perp$ and g_z predicted by tight-binding calculations. As noted in Ref. 24, however, this calculation does not account for the random orientation of the

nanocrystal axes relative to the spin-injection axis. Previous experimental work shows that anisotropic g factors should lead to a single averaged frequency in the FR data.[25] Further, the markedly different qualitative behavior of the two precession frequencies with charging in the current experiment supports the interpretation by Ref. 10 of distinct states giving rise to the components. These details favor the conclusion that g_2 is an excitonic g factor, but neither the original FR measurements nor the charging experiments give any details as to which fine-structure exciton state may be involved in the precession.

The quenching of the g_2 component can be explained within this exciton precession model by noting that in an idealized QD, selection rules dictate that circularly polarized pump pulses can only interact with a subset of singly charged QDs in the ensemble. When the single $1S_e$ electron is spin up (down), only $\sigma^+(\sigma^-)$ polarized pump pulses can be absorbed.[18] Since the $1S_e$ electrons of the resulting charged exciton must be in a singlet state, the delayed probe pulse cannot interact with the pumped QDs [Fig. 4(e)]. Thus, the FR signal from a charged QD ensemble is likely due to QDs which had no initial charge and were optically excited, or singly charged QDs which have not absorbed the pump pulse because the $1S_e$ charge has the opposite spin required for the pump helicity. For a V_{cell}, where QDs are at least singly charged, the probe pulse will not measure any QDs with optically generated excitons, but rather only those with a single electrically injected $1S_e$ electron [Fig. 4(f)]. Hence, for V_{cell} corresponding to a charged ensemble, only electron-spin precession is observed whereas exciton precession is quenched.

In summary, we have studied the effects of electrochemical charging on the spin dynamics of optically injected carriers in colloidal CdSe quantum dots. The charging of the nanocrystals suppresses the higher of two spin precession frequencies, which is most likely of an excitonic nature. Further, the amplitude of the spin precession increases up to near the half-filling potential and decreases in completely charged dots, likely due to surface defects and Pauli blocking. Inhomogeneous dephasing limits interpretation of spin-coherence times, though there is evidence for an increase in transverse electron-spin lifetime.

We thank J. Berezovsky for illuminating discussions. This work was supported by DARPA and the NSF. N.P.S. acknowledges the Fannie and John Hertz Foundation.

[1] V. I. Klimov, A. A. Mikhailovsky, S. Xu, A. Malko, J. A. Hollingsworth, C. A. Leatherdate, H.-J. Eisler, and M. G. Bawendi, Science **290**, 314 (2000).
[2] H.-J. Eisler, V. C. Sundar, M. G. Bawendi, M. Walsh, H. I. Smith, and V. I. Klimov, Appl. Phys. Lett. **80**, 4614 (2002).
[3] M. Kazes, D. Y. Lewis, Y. Ebenstein, T. Mokari, and U. Banin, Adv. Mater. (Weinheim, Ger.) **14**, 317 (2002).
[4] J. N. Cha, M. H. Bartl, M. S. Wong, A. Popitsch, T. J. Deming, and G. D. Stucky, Nano Lett. **3**, 907 (2003).
[5] M. C. Schlamp, X. G. Peng, and A. P. Alivisatos, J. Appl. Phys. **82**, 5837 (1997).
[6] H. Mattoussi, L. H. Radzilowski, B. O. Dabbousi, E. L. Thomas, M. G. Bawendi, and M. F. Rubner, J. Appl. Phys. **83**, 7965 (1998).
[7] M. Bruchez, M. Moronne, P. Gin, S. Weiss, and A. P. Alivisatos, Science **281**, 2013 (1998).
[8] W. C. Chan and S. Nie, Science **281**, 2016 (1998).
[9] J. A. Gupta, D. D. Awschalom, X. Peng, and A. P. Alivisatos, Phys. Rev. B **59**, R10 421 (1999).
[10] J. A. Gupta, D. D. Awschalom, A. L. Efros, and A. V. Rodina, Phys. Rev. B **66**, 125307 (2002).
[11] C. Wang, M. Shim, and P. Guyot-Sionnest, Science **291**, 2390 (2001).
[12] P. Guyot-Sionnest and C. Wang, J. Phys. Chem. B **107**, 7355 (2003).
[13] C. Wang, B. L. Wehrenberg, C. Y. Woo, and P. Guyot-Sionnest, J. Phys. Chem. B, **108**, 9027 (2004).
[14] L. Qu, Z. A. Peng, and X. Peng, Nano Lett. **1**, 333 (2001).
[15] S. A. Crooker, D. D. Awschalom, J. J. Baumberg, F. Flack, and N. Samarth, Phys. Rev. B **56**, 7574 (1997).
[16] U. Woggon, H. Giessen, F. Gindele, O. Wind, B. Fluegel, and N. Peyghambarian, Phys. Rev. B **54**, 17681 (1996).
[17] J. Berezovsky, M. Ouyang, F. Meier, and D. D. Awschalom, Phys. Rev. B **71**, 081309(R) (2005).
[18] A. I. Tartakovskii, M. N. Makhonin, J. Cahill, D. M. Whittaker, H-P. R. Wells, A. M. Fox, D. J. Mowbray, M. S. Skolnick, M. J. Steer, K. M. Groom, and M. Hopkinson, Appl. Phys. Lett. **85**, 2226 (2004).
[19] S. Cortez, O. Krebs, S. Laurent, M. Senes, X. Marie, P. Voisin, R. Ferreira, G. Bastard, J-M. Gerard, and T. Amand, Phys. Rev. Lett. **89**, 207401 (2002).
[20] A. Franceschetti and A. Zunger, Phys. Rev. B **62**, R16287 (2000).
[21] V. I. Klimov, D. W. McBranch, C. A. Leatherdale, and M. G. Bawendi, Phys. Rev. B **60**, 13740 (1999).
[22] J. Schrier and K. B. Whaley, Phys. Rev. B **67**, 235301 (2003).
[23] A. V. Rodina, Al. L. Efros, and A. Yu. Alekseev, Phys. Rev. B **67**, 155312 (2003).
[24] P. Chen and K. B. Whaley, Phys. Rev. B **70**, 045311 (2004).
[25] G. Salis, D. D. Awschalom, Y. Ohno, and H. Ohno, Phys. Rev. B **64**, 195304 (2001).